Self-Assembly

Deutsche Ausgabe: DOI: 10.1002/ange.201509088
Internationale Ausgabe: DOI: 10.1002/anie.201509088

Construction of Insulin 18-mer Nanoassemblies Driven by Coordination to Iron(II) and Zinc(II) Ions at Distinct Sites

*Henrik K. Munch, Jesper Nygaard, Niels Johan Christensen, Christian Engelbrekt, Mads Østergaard, Trine Porsgaard, Thomas Hoeg-Jensen, Jingdong Zhang, Lise Arleth, Peter W. Thulstrup, and Knud J. Jensen**

Abstract: *Controlled self-assembly (SA) of proteins offers the possibility to tune their properties or to create new materials. Herein, we present the synthesis of a modified human insulin (HI) with two distinct metal-ion binding sites, one native, the other abiotic, enabling hierarchical SA through coordination with two different metal ions. Selective attachment of an abiotic 2,2′-bipyridine (bipy) ligand to HI, yielding HI–bipy, enabled Zn^{II}-binding hexamers to SA into trimers of hexamers, $[[HI–bipy]_6]_3$, driven by octahedral coordination to a Fe^{II} ion. The structures were studied in solution by small-angle X-ray scattering and on surfaces with AFM. The abiotic metal ligand had a higher affinity for Fe^{II} than Zn^{II} ions, enabling control of the hexamer formation with Zn^{II} and the formation of trimers of hexamers with Fe^{II} ions. This precise control of protein SA to give oligomers of oligomers provides nanoscale structures with potential applications in nanomedicine.*

Metal-ion coordination plays a key role in protein function and self-assembly (SA).[1] Understanding and engineering protein SA is highly relevant, given its role in signaling and function. Abiotic methods to control protein SA offer the prospect of modulating their properties. Transition-metal-based SA of smaller organic compounds has enabled construction of specific 3D structures such as metal–organic frameworks.[2] Modification of peptides with metal-ion-binding ligands has enabled formation of 3D collagen networks.[3] Examples of linear protein assemblies using a single metal ion type include a streptavidin protein network with a preorganized terpyridine–biotin linker,[4] and the polymerization of a heme protein.[5] Another approach is to use native metal-ion-coordinating amino acids to link protein surfaces. Examples include model systems with cytochrome c together with proteins such as ferritin,[6] T4 lysozyme and maltose-binding protein,[7] the monomeric Rab4-binding domain of rabenosyn,[8] and Ni^{II}-directed formation of glutathione S transferase (GST) nanorings.[9] Transition-metal coordination was used in enzyme de novo design,[10] for example, in an artificial metalloenzyme combining Zn^{II} and Hg^{II} ions.[11] De novo design has combined 2,2′-bipyridine (bipy) with a native-like Cu-binding site in a three-helix bundle metalloprotein.[12] In contrast, our strategy is to control protein quaternary structure by selective introduction of an abiotic metal ligand which enables SA by metal-ion coordination.[13]

Human insulin (HI) is a protein crucial for regulating the blood glucose level. In solution, HI forms homo-oligomers depending on pH value and concentration. Two Zn^{II} ions coordinate to residue HisB10H in HI monomers forming a toroidal hexamer with a height of about 40 Å and a diameter of circa 50 Å.[14] Hexamers with Cd^{II}, Co^{II}, Ni^{II}, Cu^{II}, Mn^{II}, Fe^{II}, and Co^{III} ions were observed.[15,16] Control of HI SA and disassembly is essential for tuning the therapeutic profile. Introduction of an additional Zn^{II} binding site using natural side chains in the interprotein interface gave a "slow-release" insulin hexamer.[17] Among commercial long-acting insulins, insulin degludec[18] employs fatty diacid derivatization for formation of multihexamers and albumin binding, whereas insulin glargine incorporates pI-engineering (pI = isoelectric point) for subcutaneous precipitation. We have previously attached a metal-ion ligand derived from bipy to the B9D/B27E human insulin variant (InsX2), which is mono-/dimeric at physiological pH values.[19] With Fe^{II} ions, InsX2–bipy self-assembled into a trimer.[20]

We herein report hierarchical SA enabled by covalent attachment of abiotic bipy at the LysB29 residue of native HI (see Figure S1 in the Supporting Information) and coordination with two physiologically relevant metal ions. Our aim was to combine native hexamer formation with Zn^{II} and the abiotic trimerization around an Fe^{II} ion to yield a HI with new oligomerization properties controlled by the Fe^{II} concentration. Zn^{II} and Fe^{II} ions are among the most abundant metal ions in natural protein interfaces.[21] They have distinct affinities for the attached abiotic metal ligand (bipy). Addition of only Zn^{II} ions gave predominantly HI–bipy hexamers (Figure 1, equilibrium ii), whereas addition of only Fe^{II} ions resulted in the formation of a large uncontrolled network (Figure 1, equilibrium i). However, the presence of both metal ions simultaneously gave rise to the formation of trimers of hexamers ($[[HI–bipy]_6]_3$; Figure 1, equilibrium iii). This is, to our knowledge, the first time metal-ion-responsive

[*] Dr. H. K. Munch, Dr. N. J. Christensen, M. Østergaard, Prof. Dr. P. W. Thulstrup, Prof. Dr. K. J. Jensen
Department of Chemistry
University of Copenhagen (Denmark)
E-mail: kjj@chem.ku.dk
J. Nygaard
MAX-lab, Lund University (Sweden)
Dr. T. Porsgaard, Dr. T. Hoeg-Jensen
Novo Nordisk A/S, 2760 Maaloev (Denmark)
J. Nygaard, Prof. Dr. L. Arleth
Niels Bohr Institute, University of Copenhagen (Denmark)
Dr. C. Engelbrekt, Prof. Dr. J. Zhang
Department of Chemistry, Technical University of Denmark
Kgs. Lyngby (Denmark)

Supporting information for this article (including the Experimental Section) is available on the WWW under http://dx.doi.org/10.1002/anie.201509088.

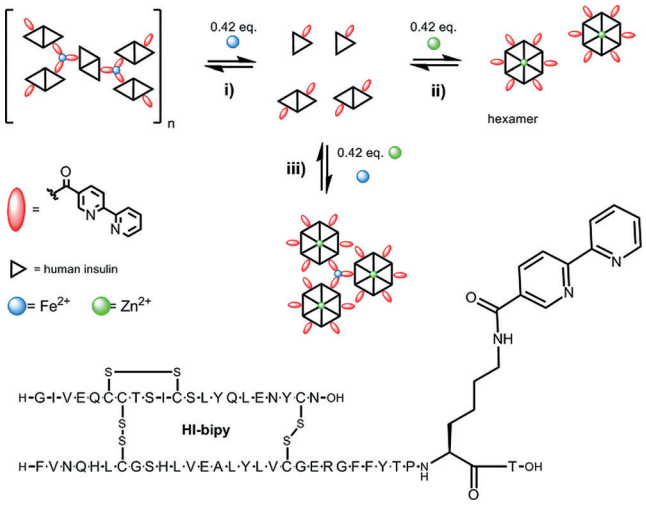

Figure 1. HI–bipy oligomers (top) and the ligand structure (bottom). Fe^{II} ions preferentially coordinate to bipy (i), whereas HI–bipy forms hexamers in the presence of Zn^{II} ions (ii). Combining Fe^{II} and Zn^{II} ions gave a stable 18-mer (iii).

protein SA was achieved by combining native and non-native SA. Intravenous (iv) administration of HI–bipy in rats lowered blood glucose, pointing towards its use in slow-release formulations (Section S7 in the Supporting Information).

HI–bipy (500 μM) in solution was studied by small-angle X-ray scattering (SAXS)[20,22] with 2.5 equivalents of Zn^{II} ions per hexamer (Figure 2), that is, a small excess compared to the required two Zn^{II} ions per hexamer. Insulin hexamer presence is highly characteristic in the shape of the SAXS I(q) curve (Figure 2, dark-blue curve). The SAXS data were analyzed by superposition on native HI results (Figure 2).

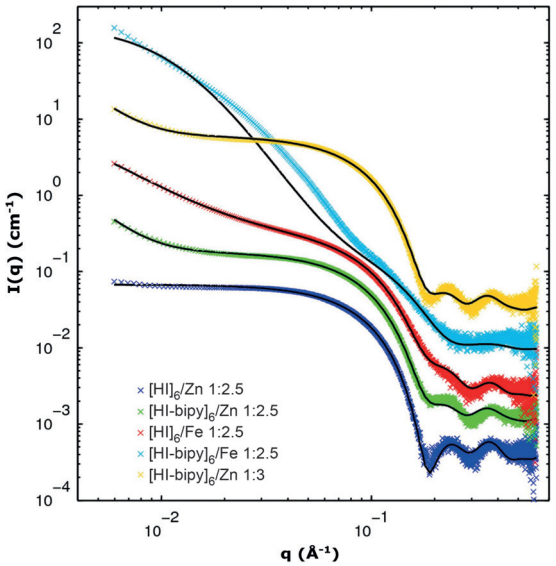

Figure 2. SAXS data (colored data) and model fits (black lines). For clarity the data and fits have been vertically displaced. The dark-blue data set is on the absolute scale. The shape of the scattering curve, including the ripples at $q = 0.24$ Å^{-1} and $q = 0.37$ Å^{-1}, are characteristic of the insulin hexamer.

Relative to HI, the yield of hexamer formation for HI–bipy in the presence of 2.5 and 3.0 equivalents of Zn^{II} per hexamer was about 80 % and 90 %, respectively. Thus, insulin hexamer formation was largely retained after attachment of bipy at LysB29.

HI hexamers also formed with 2.5 equivalents of Fe^{II} ions per hexamer, although to a lower extent (66 %; Figure 2, red curve; Figure S6). Interestingly, no hexamers were detected for HI–bipy with Fe^{II} ions which gave oligomers of trimers, $[[HI–bipy]_3]_n$ (Figure 1; Figure 2, cyan curve). Upon addition of Fe^{II} ions to HI–bipy, the color of the samples turned magenta, characteristic of $[Fe(bipy)_3]^{2+}$ coordination, and in the absence of Zn^{II} ions a precipitate formed, indicating the formation of larger aggregates.

The selectivity of Zn^{II} and Fe^{II} indicated a way to construct well-defined oligomers of HI hexamers. Zn^{II} ions would coordinate primarily to the His residue in HI, forming hexamers, whereas the Fe^{II} ion concentration would control the degree of formation of trimers of hexamers. Here, 2.5 equivalents of Zn^{II} ions per HI–bipy hexamer gave circa 80 % hexamers, which remained constant regardless of the co-added Fe^{II} concentration (Figure S4), underlining the selectivity of Fe^{II} for bipy over the native HI metal-binding sites. Furthermore, the fraction of trimers of hexamers increased with Fe^{II} concentration, and the SAXS $I(q)$ shape characteristic of the insulin hexamer was present at all Fe^{II} concentrations (Figure S4). This showed successful formation of primarily trimers of insulin hexamers (that is, 18-mers or $[[HI–bipy]_6]_3$). From SAXS measurements, it was clear that the 18-mers were disc-like structures with a radius of about 40 Å. As the Fe^{II} concentration was increased to Fe^{II}/HI–bipy 1:6, even larger HI–bipy hexamer assemblies formed.

The coordination of Fe^{II} ions to bipy was also confirmed by UV/Vis absorption spectroscopy with the appearance of an absorption band at $\lambda = 550$ nm. This band increased with increasing Fe^{II} concentration (Figure S7), proving that Fe^{II} ion coordination to surface-exposed bipy on the hexamers caused the oligomerization. Circular dichroism (CD) measurements of these samples showed exciton bands at $\lambda = 300$ nm and 550 nm (Figure S8), indicating that Fe–bipy trimers were formed enantioselectively. The Cotton signature of the bands showed a stereochemical preference for a Δ configuration, which was opposite to that for the monomeric InsX2–bipy analogue modified at the corresponding Lys residue.[15] CD temperature denaturation at various Fe^{II} concentrations showed similar secondary structure stability for HI–bipy and HI. Rewardingly, preliminary data indicated that HI–bipy had a delayed onset of fibrillation in a thioflavin assay (data not shown).

Importantly, the SA of trimers of hexamers was reversible. Excess ethylenediaminetetraacetic acid (EDTA) caused the intensity of the absorbance band at $\lambda = 550$ nm to decrease in the Fe^{II}-loaded samples, as a result of disassembly of the $[Fe(bipy)_3]^{2+}$ complex and thus of the trimers of HI–bipy hexamers (Section S6).

Finally, SA of HI–bipy (200 μM) was studied by AFM at higher Fe^{II} concentration. Native HI with Zn^{II} and/or Fe^{II} did not form any superstructures beyond the hexamer, whereas HI–bipy in the presence of both Zn^{II} and Fe^{II} ions formed

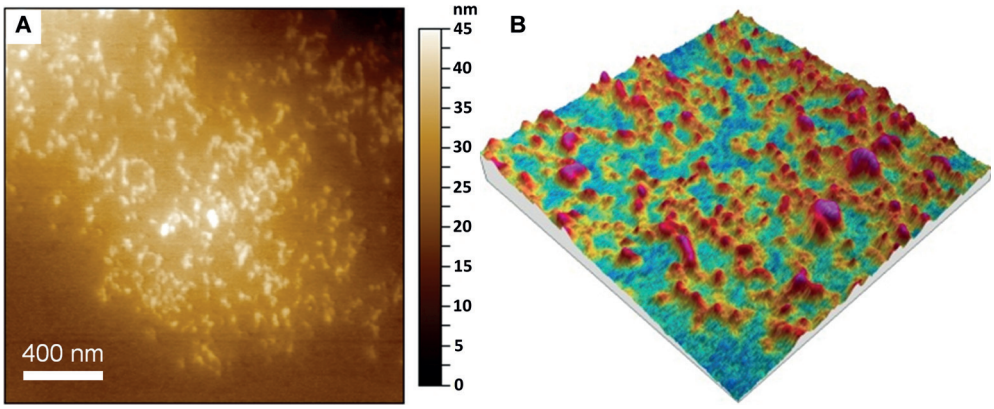

Figure 3. AFM images for a HI–bipy (200 μM) sample in the presence of Zn^{II} and Fe^{II} ions (100 μM of both). A) Topography image (scan range = 2 μm) of hexamer networks. B) Magnified view of hexamer networks presented as a combined 3D plot where topography is shown as a 3D surface and the phase contrast is shown using a range of colors (scan range = 1 μm).

oligomers of hexamers. AFM images for the HI–bipy sample on a mica surface are shown in Figure 3 (and Section S4). Statistical analysis of heights gave three groups at 4.1 ± 0.7, 5.6 ± 0.4 and 7.3 ± 0.7 nm (Figure S12). The first two groups agree well with the dimensions of the insulin hexamer. These measurements thus correspond to different orientations of the hexamer moiety in the self-assembled structure on the mica surface. The third height group, 7.3 ± 0.7 nm, roughly corresponds to two hexamer diameters, and may indicate two closely associated hexamer moieties protruding from the surface. AFM also provided some quantification of the regularity of the surface self-assembled structure by showing a tendency for height maxima to occur at in-plane distances of 40 ± 10 nm.

Molecular modeling (Section S5) was used to further analyze the surface SA detected by AFM. A minimal model consistent with the experimental detection of trimeric Fe^{II} bipy complexes is $[[HI–bipy]_6]_3$, shown as the central part (dark green) of the larger oligomer in Figure 4. The hypothetical 9-mer of hexamers $[[HI–bipy]_6]_9$ in the figure was built by adding two hexamers (shown in blue) complexed through an Fe^{II} ion to an exposed, symmetry-related bipy ligand on each hexamer of the central $[[HI–bipy]_6]_3$. Figure 4 shows approximate length scales that are expected for oligomeric networks of HI–bipy hexamers. Assuming that the structure in Figure 4A shows the surface viewed from above, the side view in Figure S14C shows how a height of about 11 nm may arise as a result of the particular arrangement of the hexamers (blue) associating with the central trimer of hexamers (dark green). Surface-protein interactions may limit actual heights to the approximate value of 7 nm detected with AFM.

In summary, we have shown the controlled SA of trimers of insulin hexamers, $[[HI–bipy]_6]_3$, and higher oligomers by attaching a metal ligand (bipy) to HI. By combining the inherent ability of HI to form stable hexamers with divalent metal ions and the affinity of bipy for Fe^{II} ions, the system formed either hexamers or a larger network when the metal ions were added separately. Simultaneous addition of Zn^{II} and Fe^{II} ions gave insulin 18-mers as trimers of hexamers and higher oligomers depending on the Fe^{II} concentration. The SA was shown to be reversible, as addition of EDTA caused disassembly of higher oligomers. The metal-ion-mediated control of protein SA uses abiotic ligands with suitable directionality that can yield 3D networks and thus opens the possibility for the design and preparation of specific protein architectures on the nanoscale. We envision that such protein nanostructures may potentially find application in the controlled release of biopharmaceuticals from subcutaneous depots.

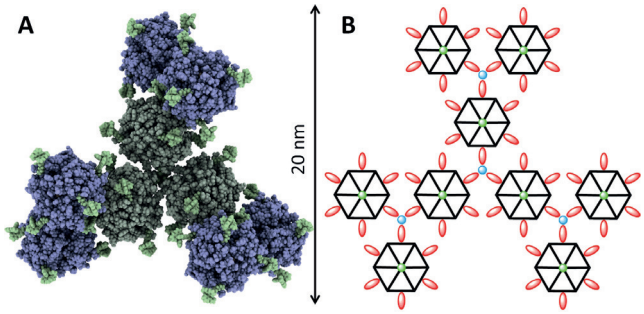

Figure 4. Molecular model of a HI–bipy 54-mer. The 54-mer is formed by the complexation of a central trimer of hexamers (dark green) with three sets of two hexamers (blue). An exposed bipy on each hexamer of the central tri-hexamer coordinates to an Fe^{II} center, which is also coordinated (with a Δ-*fac* configuration) to one free bipy on each hexamer of the hexamer pair. A) Top view, B) 2D representation. Bipy sites in (A) are shown as Fe^{II}–bipy complexes, indicating the potential position of additional HI–bipy units attached to the B29 residue in larger oligomers.

Acknowledgements

We gratefully acknowledge beamtime at beamline ID14-3 at the ESRF, the excellent support provided by Dr. A. Round, and Villum Fonden (BioNEC) for funding.

Keywords: atomic force microscopy · insulin · nanostructures · self-assembly · small-angle X-ray scattering

How to cite: *Angew. Chem. Int. Ed.* **2016**, *55*, 2378–2381
Angew. Chem. **2016**, *128*, 2424–2427

[1] E. Permyakov, *Metalloproteomics*, Wiley, Hoboken, **2009**.
[2] H.-C. Zhou, J. R. Long, O. M. Yaghi, *Chem. Rev.* **2012**, *112*, 673.
[3] a) T. Koide, M. Yuguchi, M. Kawakita, H. Konno, *J. Am. Chem. Soc.* **2002**, *124*, 9388; b) D. E. Przybyla, J. Chmielewski, *J. Am.*

Chem. Soc. **2008**, *130*, 12610; c) M. M. Pires, J. Chmielewski, *J. Am. Chem. Soc.* **2009**, *131*, 2706; d) M. M. Pires, D. E. Przybyla, J. Chmielewski, *Angew. Chem. Int. Ed.* **2009**, *48*, 7813; *Angew. Chem.* **2009**, *121*, 7953.
[4] S. Burazerovic, J. Gradinaru, J. Pierron, T. R. Ward, *Angew. Chem. Int. Ed.* **2007**, *46*, 5510; *Angew. Chem.* **2007**, *119*, 5606.
[5] H. Kitagishi, K. Oohora, H. Yamaguchi, H. Sato, T. Matsuo, A. Harada, T. Hayashi, *J. Am. Chem. Soc.* **2007**, *129*, 10326.
[6] D. J. E. Huard, K. M. Kane, F. A. Tezcan, *Nat. Chem. Biol.* **2013**, *9*, 169.
[7] A. Laganowsky, M. Zhao, A. B. Soriaga, M. R. Sawaya, D. Cascio, T. O. Yeates, *Protein Sci.* **2011**, *20*, 1876.
[8] B. S. Der, M. Machius, M. J. Miley, J. L. Mills, T. Szyperski, B. Kuhlman, *J. Am. Chem. Soc.* **2011**, *133*, 375.
[9] Y. Bai, Q. Luo, W. Zhang, L. Miao, J. Xu, H. Li, J. Liu, *J. Am. Chem. Soc.* **2013**, *135*, 10966.
[10] M. L. Zastrow, V. L. Pecoraro, *Coord. Chem. Rev.* **2013**, *257*, 2565.
[11] M. L. Zastrow, A. F. A. Peacock, J. A. Stuckey, V. L. Pecoraro, *Nat. Chem.* **2011**, *3*, 118.
[12] M. R. Ghadiri, M. A. Case, *Angew. Chem. Int. Ed. Engl.* **1993**, *32*, 1594; *Angew. Chem.* **1993**, *105*, 1663.
[13] K. J. Jensen, *Pept. Sci.* **2013**, *19*, 537.
[14] R. Palmieri, R. W. K. Lee, M. F. Dunn, *Biochemistry* **1988**, *27*, 3387.
[15] a) J. Schlichtkrull, *Acta Chem. Scand.* **1956**, *10*, 1455; b) M. C. Storm, M. F. Dunn, *Biochemistry* **1985**, *24*, 1749.
[16] P. Kurtzhals, B. Kiehr, A. R. Sørensen, *J. Pharm. Sci.* **1995**, *84*, 1164.
[17] N. B. Phillips, Z.-l. Wan, L. Whittaker, S.-Q. Hu, K. Huang, Q.-x. Hua, J. Whittaker, F. Ismail-Beigi, M. A. Weiss, *J. Biol. Chem.* **2010**, *285*, 11755.
[18] I. Jonassen, S. Havelund, T. Hoeg-Jensen, D. B. Steensgaard, P.-O. Wahlund, U. Ribel, *Pharm. Res.* **2012**, *29*, 2104.
[19] H. K. Munch, S. T. Heide, N. J. Christensen, T. Hoeg-Jensen, P. W. Thulstrup, K. J. Jensen, *Chem. Eur. J.* **2011**, *17*, 7198.
[20] J. Nygaard, H. K. Munch, P. W. Thulstrup, N. J. Christensen, T. Hoeg-Jensen, K. J. Jensen, L. Arleth, *Langmuir* **2012**, *28*, 12159.
[21] P. A. Sontz, W. J. Song, F. A. Tezcan, *Curr. Opin. Chem. Biol.* **2014**, *19*, 42.
[22] a) D. I. Svergun, M. H. J. Koch, *Rep. Prog. Phys.* **2003**, *66*, 1735; b) C. L. P. Oliveira, T. Vorup-Jensen, C. B. F. Andersen, G. R. Andersen, J. S. Pedersen, *Lect. Notes Phys.* **2009**, *776*, 231; c) R. Høiberg-Nielsen, P. Westh, L. K. Skov, L. Arleth, *Biophys. J.* **2009**, *97*, 1445.

Received: September 28, 2015
Revised: December 1, 2015
Published online: January 14, 2016

